Electronic Supporting Information

Stable Sn^{2+} Doped $FAPbI_3$ Nanocrystals for Near-infrared LED

Raihana Begum,[†] Xin Y. Chin, [†] Mingjie Li,[‡]Bahulayan Damodaran, [†] Tze C. Sum,[‡] Subodh Mhaisalkar,[†,§] and Nripan Mathews [†,§]*

[†] Energy Research Institute @ NTU (ERI@N), Nanyang Technological University, Research Techno Plaza, X-Frontier Block, Level 5, 50 Nanyang Drive, 637553, Singapore

[‡] Department of Physics and Applied Physics, School of Physical and Mathematical Sciences, Nanyang Technological University, 21 Nanyang Link, SPMS-PAP 03-05, Singapore 637371

[§] School of Materials Science and Engineering, Nanyang Technological University, 50 Nanyang Avenue, Singapore 639798

Experimental Section

Chemicals: Propionic acid (ACS grade reagent, >99.5%), formamidine acetate (99%), toluene (anhydrous, 99.8%), 1-octadecene (tech. grade, 90%), lead iodide (99.999%, perovskite grade), oleic acid (reagent grade, 99%) oleylamine (tech. grade, 70%). All chemicals are purchased from Sigma-Aldrich. Octadecene, oleic acid and oleylamine were dried at 150 0C, with continuous stirring, under vacuum condition for about 3 h. Purged N2 gas, before we store it as such for further uses.

Synthesis of $FAPbI_3$ Nanocrystals: The nanocrystals were synthesized following a method reported by Protesescu et al.[1] However, we used formamidine propionate (FA-PA) instead of FA-oleate. The first step involves synthesis of FA-PA. About 5 ml of propionic acid is added to 0.26 g of formamidinium acetate and continuously stirred at 80 ^{0}C for about 30 minutes.

Synthesis of undoped $FAPbI_3$ NCs: About 5 ml of dried octadecene is added to PbI_2 (0.086 g) taken in a 2-neck round bottom flask. About 1 mL of dried oleic acid and 650 uL of dried oleylamine are injected to the reaction flask in vacuum condition. Heating at 120 0C for about 1 h follows this. When PbI_2 dissolves completely, the temperature is reduced to 75 ^{0}C. At that temperature, 1 ml of FA-propionate (pre-heated to 80 ^{0}C) is injected. The reaction flask is immediately transferred to an ice-water bath.

Synthesis of Sn^{2+}-doped $FAPbI_3$ NCs: For Sn doping, we used three different concentrations of tin iodide. Both Sn and Pb iodide are added together, along with 5 ml of octadecene, 1 ml of oleic acid and 650 uL of oleylamine. The rest is similar to the synthesis and purification of undoped NCs.

Isolation and Purification: The NCs in octadecene were centrifuged at 8000 RPM. The precipitate is collected and re-dispersed in 10 mL of anhydrous toluene. The NCs are then washed with anti-solvent, acetonitrile (toluene: acetonitrile= 2:1), centrifuged again at 8000 RPM. The pellet obtained is re-dispersed in 10 mL of anhydrous toluene. Centrifuged once again at 3000 RPM to discard the bigger particles. The top part is used for further characterizations.

For LED device fabrication, the pellet obtained after acetonitrile washed, is re-dispersed in 1 mL of anhydrous toluene and centrifuged at 3000 RPM. The pellet formed is discarded and used the top part as ink.

Characterizations: The UV-visible and PL spectra of the NCs were collected using Shimadzu UV1800 Spectrophotometer and FluoroMax-4 spectrofluorophotometer, respectively. Powder XRD patterns were recorded in a XRD Bruker D8 Advance in thin film mode. The average sizes of the NCs were determined by using a Tecnai transmission electron microscope (TEM, model FEI Tecnai F20). For powder XRD measurements, the NCs in toluene are deposited on a glass substrate and for TEM on a carbon-coated copper grid. ICP-OES (Inductively coupled plasma - optical emission spectrometry) measurement was

done using Perkin Elmer Optima 7300DV instrument, samples were digested with acid before measurement. FTIR measurement was done using JACO FT/IR – 6700 spectrophotometer. XPS measurements were done using a pass energy of 26 eV and 0.1 eV per step. The XPS instrument model used is Quantera II from Ulvac-Phi. The absolute PLQY was measured with the sample in an integrating sphere using 400 nm laser excitation and the emission was collected with charge-coupled device array (Princeton Instruments, Pixis) coupled to a monochromator (Acton, Spectra Pro). Time-resolved PL was performed using a streak camera system (Optronis Optoscope). The 400 nm pump pulse laser was generated by frequency doubling the 800 nm laser from the regenerative amplifier (Coherent Libra, pulse width 50 fs, repetition rate 1kHz) using a BBO crystal.

Device fabrication: As-purchased indium-tin oxide (ITO; Pre-etched, sheet resistance ~8 Ω cm^{-1}; Wuhan Jinge Solar Energy Technology Co., Ltd) glass substrates were used for device fabrication. The ITO glass substrates were washed in detergent solution, acetone, ethanol, and 2-propanol in an ultrasonication bath, followed by drying and treatment under UV-ozone for 20 min. The hole transporting layer, PEDOT:PSS (Clevios 4083; filtered with 0.45 μm PVDF filter) was then spin-coated at 4000 rpm for 1 min and thermally annealed at 130 °C for 10 min to remove any residual solvent. The substrates were then transferred to an argon-filled glovebox for the spin coating of emitter layer. The Sn-doped $FAPbI_3$ NCs inks were spin-coated at 500 rpm for 1 min on top of the PEDOT:PSS [poly(3,4-ethylenedioxythiophene) polystyrene sulfonate] layer. Followed by thermal evaporation of electron transporting layer (POT2T, 2,4,6-Tris[3-(diphenylphosphinyl)phenyl]-1,3,5-triazine) of thickness 45 nm under high vacuum (10-6 torr). Finally, thermal evaporation of electrode materials Calcium (7 nm) and Aluminium (80 nm) using a metal shadow mask, to define the device active area of 3 mm^2.

Device characterization: Prior to electroluminescence characterization, all LED devices were encapsulated with epoxy resin and the encapsulation is done inside the argon-filled glovebox. A Keithley 2612B was used to obtain the current-voltage characteristics of the LED devices using a scan rate of 1 V

s-1 (step size 0.1 V, step interval 0.1 s). The light emission was collected by an integrating sphere (OceanOptics FOIS-1) coupled to a calibrated spectrophotometer (OceanOptics QEPro). OceanOptics HL-3 Plus vis-NIR light source, calibrated using a procedure and documentation patterned after the ISO 17025, IEC Guide 115 and JCGM100:2008 (GUM) protocols, is used to calibrate the absolute irradiance measurement of the spectrometer. As LED devices are placed on outside of the integrating sphere, only forward emission is captured while the edge emission contribution is lost outside the integrating sphere.

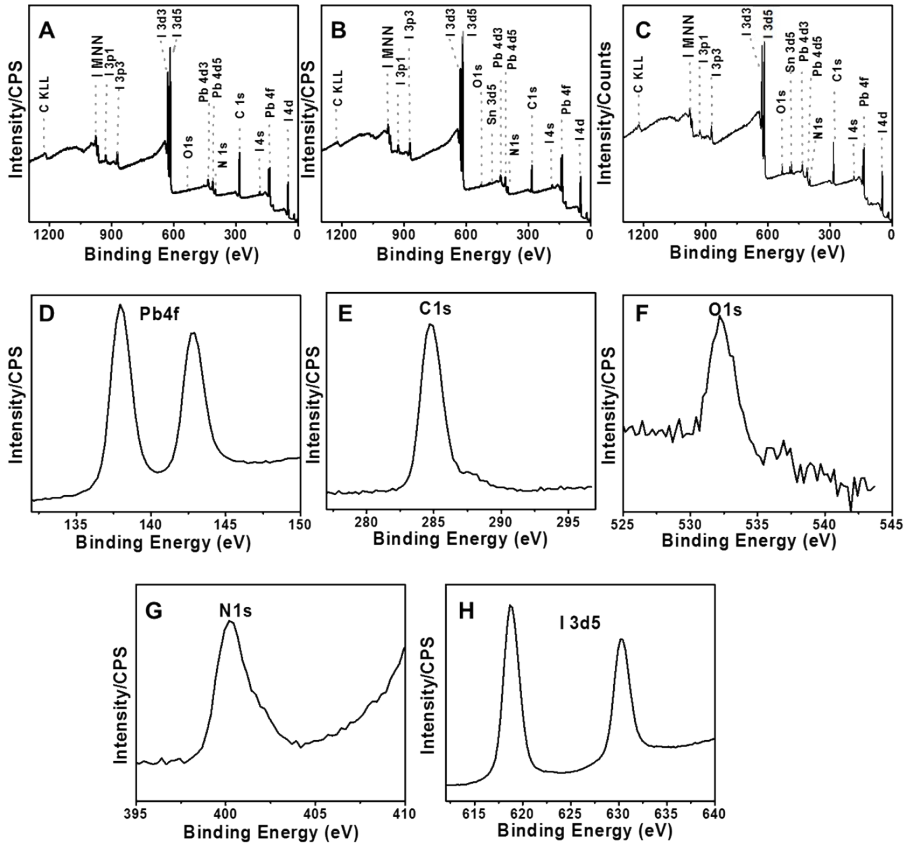

Fig. S1: Survey X-ray photoelectron spectra (XPS) of (A) undoped (B) 1.8% Sn- doped (C) 11.4% Sn-doped $FAPbI_3$ NCs. High- resolution XPS analysis corresponding to (D) Pb 4f, (E) C 1s, (d) N1s, (F) O1s (G) N1S and (H) I3d5. The high-resolution spectra were also recorded corresponding to the core levels of C1s, N1s, O1s, Pb 4f and I 3d5 for the undoped NCs and the other Sn-doped NCs and the peak positions are found to be same as of doped NCs.

Sn doped NCs with a lower concentration than 1.8% of Sn was also synthesized. The photoluminescence (PL) peak position and absorption shifts to 791 nm from 797 nm (from that of undoped NCs), however, we could not determine the exact concentration of Sn^{2+} by XPS due to below detection limit of the instrument. The PLQY and phase stability of low doped NCs also did not improve significantly.

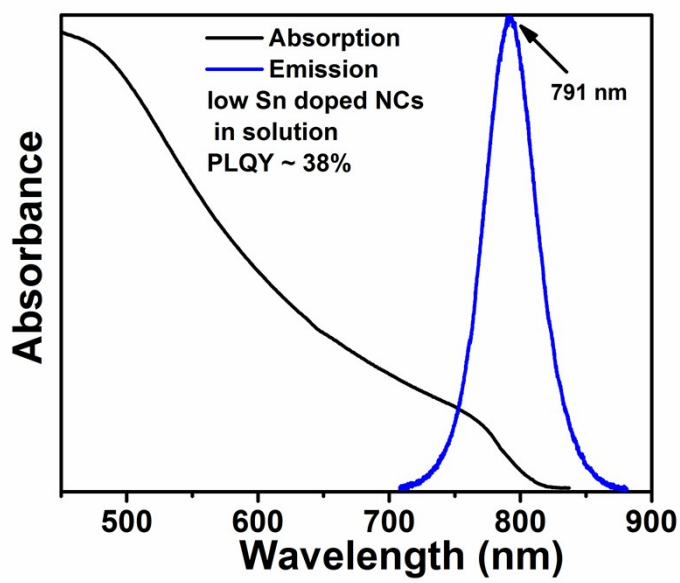

Fig. S2: Absorption and emission spectra of low doped $FAPbI_3$ NCs

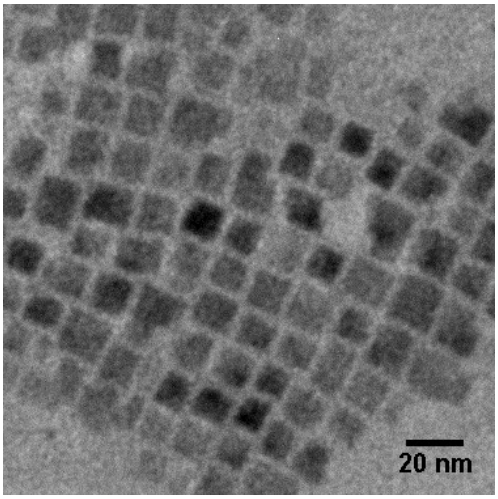

Fig. S3: TEM image of 1.8% Sn-doped $FAPbI_3$ NCs

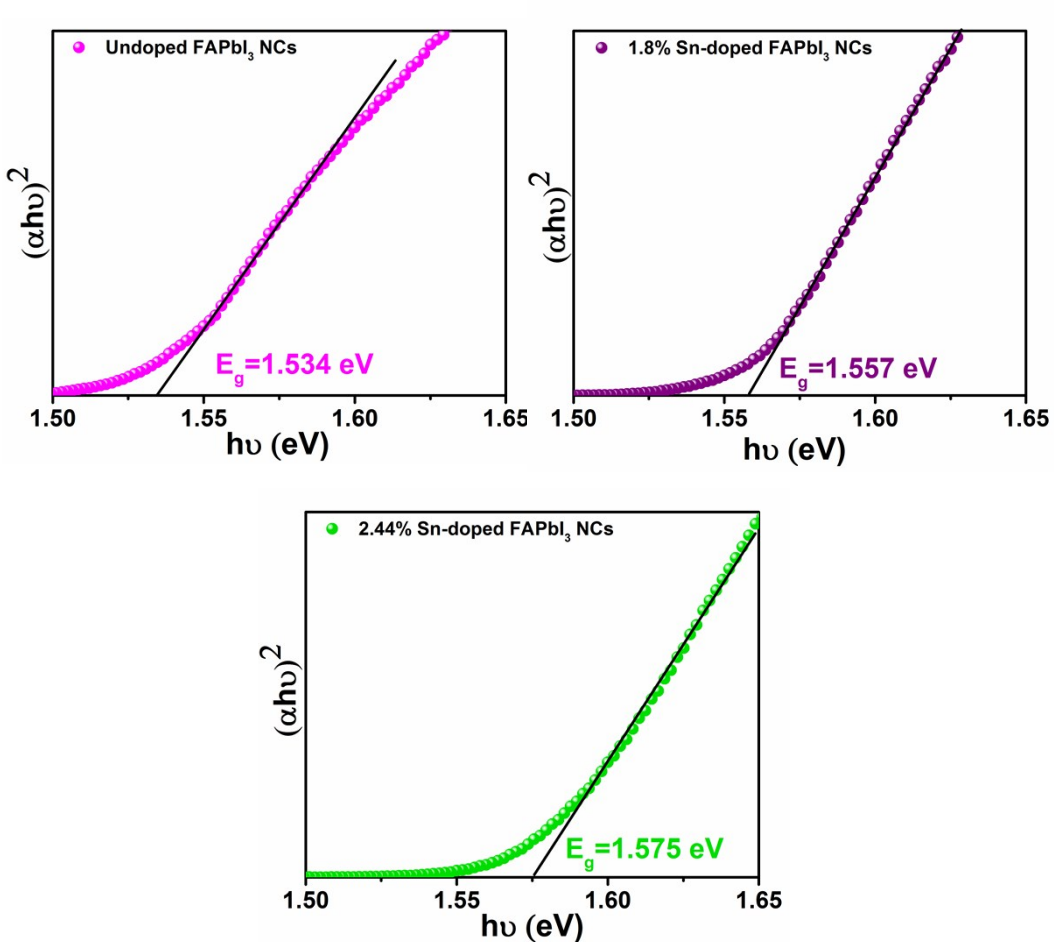

Fig. S4: Tauc Plot of undoped $FAPbI_3$ NCs and those doped with different percentage of Sn^{2+}.

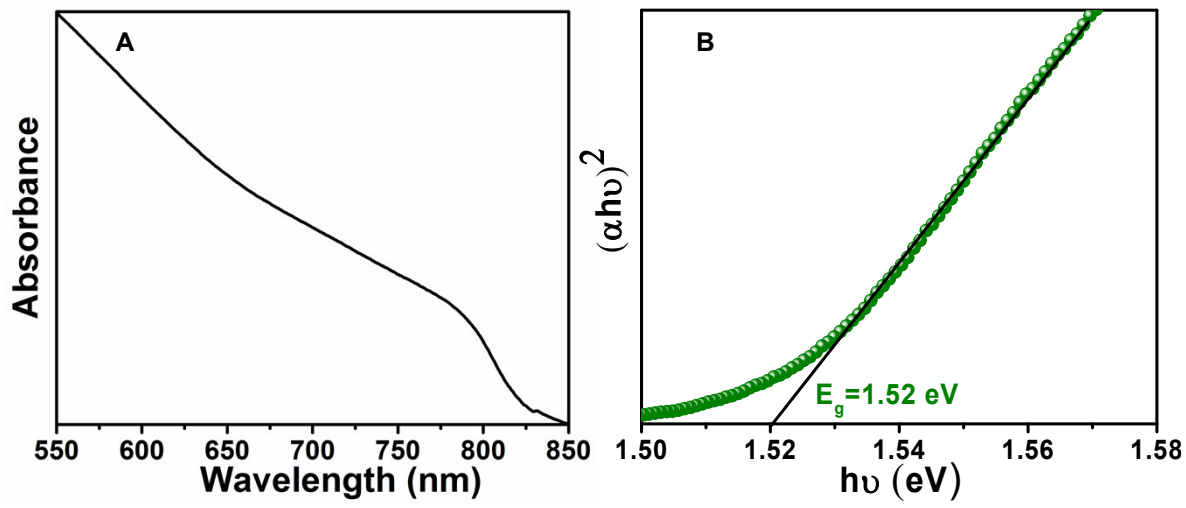

Fig. S5: (A) Absorption spectrum (B) Tauc plot of 11.4% Sn-doped $FAPbI_3$ NCs.

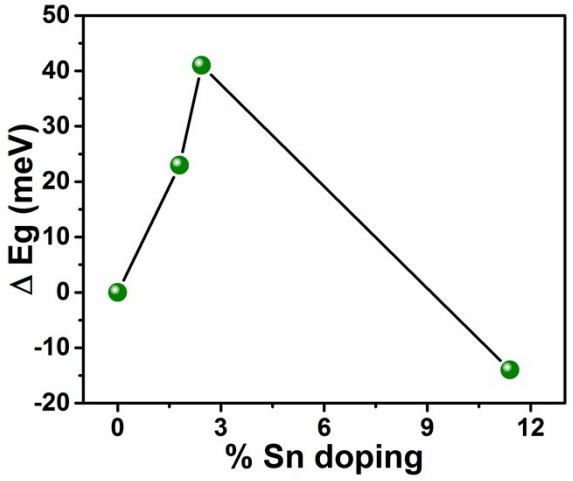

Fig. S6: Energy difference, ΔE (meV) versus % Sn-doping in $FAPbI_3$ NCs.

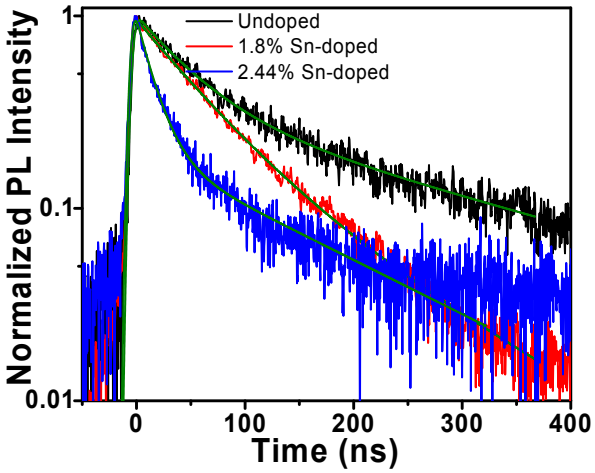

Fig. S7: Time-resolved PL decays of undoped and Sn-doped $FAPbI_3$ NCs with bi-exponential fitings (green solid lines).

The radiative emission lifetime (τ_{rad}) and the non-radiative recombination lifetime ($\tau_{non\text{-}rad}$) have the following relationships with the measured PL lifetime (τ_{PL}):

$$\tau_{rad} = \tau_{PL}/\Phi, \text{ and } \tau_{non\text{-}rad} = \tau_{PL}/(1\text{-}\Phi), \text{ where } \Phi \text{ is the PLQY.}$$

We therefore can obtain the average radiative lifetime ($\tau_{rad\text{-}avg}$) and average non-radiative lifetime ($\tau_{non\text{-}rad\text{-}avg}$) based on the average measured PL lifetime [$\tau_{PL\text{-}avg}=(a_1*t_1+a_2*t_2)/(a_1+a_2)$], where a_1, a_2, t_1 and t_2 are amplitudes and the fitted lifetimes by bi-exponential decay function.

Table S1: Time resolved PL decay fitting parameters, decay lifetimes (t_i) and the related amplitudes (a_i). Also, calculated τ_{rad} and $\tau_{non\text{-}rad}$ are listed.

sample	PLQY	t_1(ns)	a_1	t_2 (ns)	a_2	$\tau_{PL\text{-}avg}$	τ_{rad}	$\tau_{non\text{-}rad}$
undoped	35%	48	0.69	278	0.31	119.3	340.8	183.5
1.8% Sn doped	63%	40	0.78	132	0.22	60.24	95.6	162.8
2.44% Sn doped	46%	16	0.85	154	0.15	36.7	79.8	68.0

The observed shorter emission lifetime does not necessarily imply the more non-radiative traps in the sample. Similar observations were reported in perovskite core/shell octyl-ammonium lead bromide nanomaterials over $MAPbBr_3$ NCs core and in Sn-doped $MAPbBr_3$ NCs.[2-4] In Sn- doped $MAPbBr_3$ NCs, PLQY increased from 40% to 80%, while both lifetime component (t_1 and t_2) decreases.[3]

Table S1 shows that the Sn doped samples have shorter $\tau_{non\text{-}rad}$, which means reduction of non-radiative pathways. The radiative emission decay also become faster, i. e. radiative decay rate constant become larger.

According to Fermi's golden rule, the radiative decay rate of spontaneous emission in the dipole approximation is given by

$1/\tau_{rad} = \varpi^3 n^3 \langle \mu_{12} \rangle^2 / 3\pi\varepsilon_0 \hbar c^3$, where ϖ is the emission frequency, n is the index of refraction, $\langle \mu_{12} \rangle$ is the transition dipole moment.

(according to B. Henderson and G. Imbusch, Optical Spectroscopy of Inorganic Solids (Clarendon Press, Oxford, UK, 1989))

Our observation of increased radiative decay rate in Sn doped NCs can thus be explained by the Fermi's rule as the emission blue-shifted after Sn-doping. And also, the increased PLQY is due to the increased radiative rate constant.

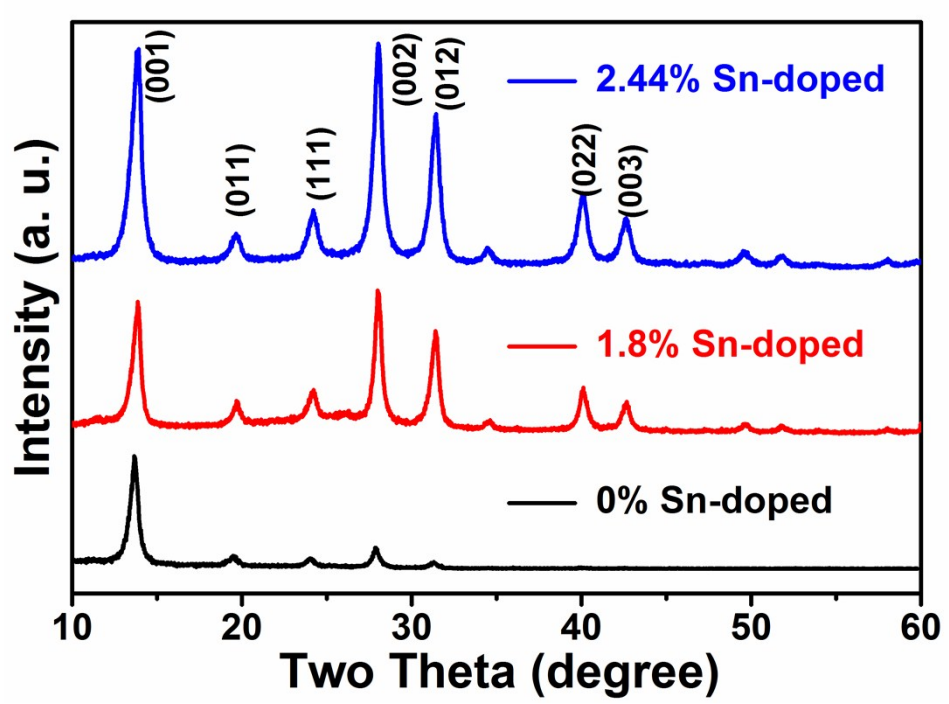

Fig. S8: Powder XRD patterns of undoped $FAPbI_3$ NCs, 1.8% Sn-doped and 2.44% Sn-doped $FAPbI_3$ NCs.

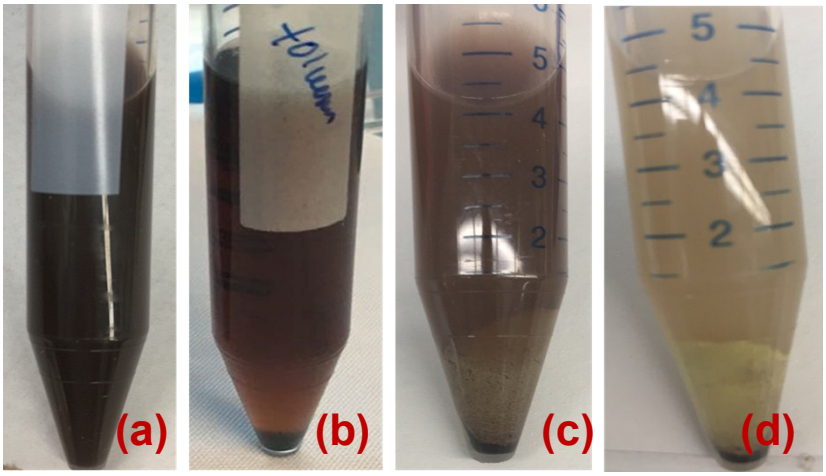

Fig. S9: Photographs of undoped $FAPbI_3$ NCs washed with acetonitrile and then dispersed in toluene and stored under ambient condition (a) Day 1 (b) Day 2, samples got precipitated, no phase degradation was observed (c) Day 3, phase degradation starts from the precipitate (d) Day 3, few hours later degraded completely.

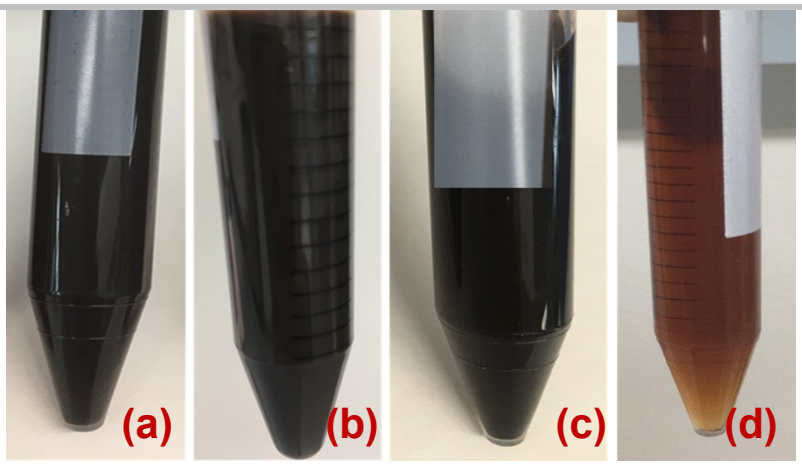

Fig. S10: Photographs of 2.44% Sn-doped $FAPbI_3$ NCs washed with acetonitrile and then dispersed in toluene and stored under ambient condition (a) Day 1 (b) Day 7 (c) One month later, slight precipitation occurs (d) more than two months, sample get precipitated, the image is of the top part, after discarding precipitate, no phase degradation was observed.

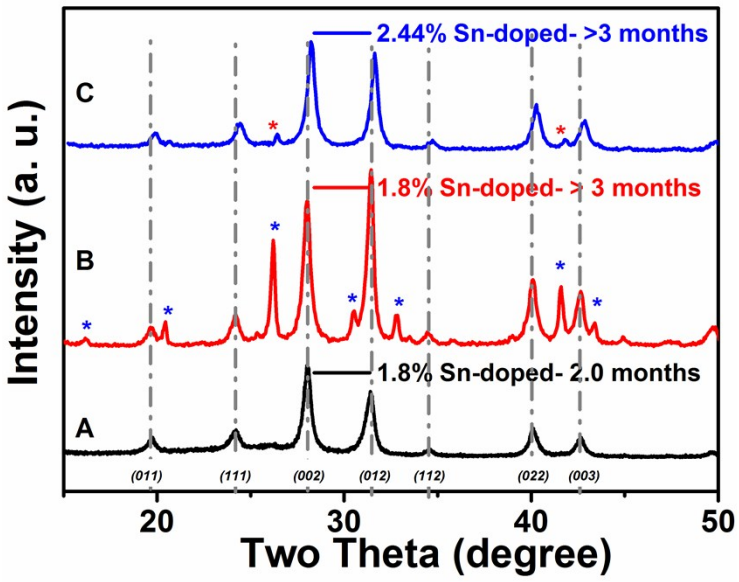

Fig. S11: XRD patterns of (A) 1.8% Sn-doped $FAPbI_3$ NCs deposited on glass substrate after 2 months of synthesis (dispersed in toluene and stored under ambient condition), showed no extra peaks; (B) the same NCs deposited after more than 3 months, showed few extra peaks (marked by blue asterisk*) that corresponds to δ-$FAPbI_3$ phase and (C) 2.44% Sn-doped $FAPbI_3$ NCs, deposited more than 3 months

after synthesis (dispersed in toluene and stored under ambient condition), showed two extra peaks (marked by red asterisk*).

Table S2: PLQY measurements of the NCs samples

Sample	PLQY (in solution)	PLQY (deposited on glass substrate)
Undoped $FAPbI_3$ NCs	35%	11%
1.8% Sn doped $FAPbI_3$ NCs	63%	28%
2.44% Sn doped $FAPbI_3$ NCs	46%	17%

FTIR measurements were performed to understand the ligand composition-percentage of propionic acid and oleic acid in our NCs. FTIR measurement was done on 1.8% Sn doped NCs, where FA-propionate was used as source of FA (formamidinium). For comparison, we also recorded FTIR spectrum of oleic acid and propionic acid, which were used as purchased.

Both the ligands are mono carboxylic acids, the characteristic C=O stretching vibration is observed at 1703 cm^{-1} with similar intensities in all the 3 samples. The vibration bands in the range 2855-2865 cm^{-1} and 2920-2930 cm^{-1} refer to the C-C and C-H stretching modes of $-CH_2-$ groups. As seen in Figure B, pure oleic acid has very strong peaks in the said region, while pure propionic acid (Figure A) has weak peaks. In the FTIR spectrum for Sn doped NCs (Figure C), where FA-propionate was used, the intensity of the alky band is significantly decreased, which indicates obvious decrease in the total carbon content of the NCs, that facilitates charge injection when used in LED devices.

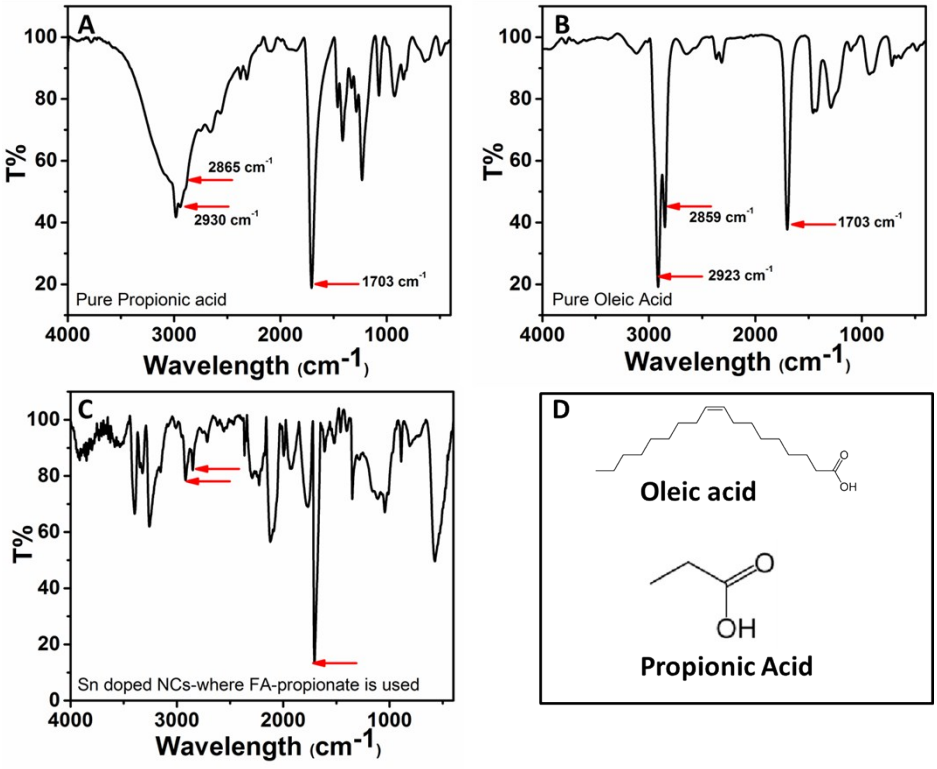

Fig. S12: FTIR spectra of (A) propionic acid (B) oleic acid (C) Sn doped NCs (D) chemical formula of the ligands

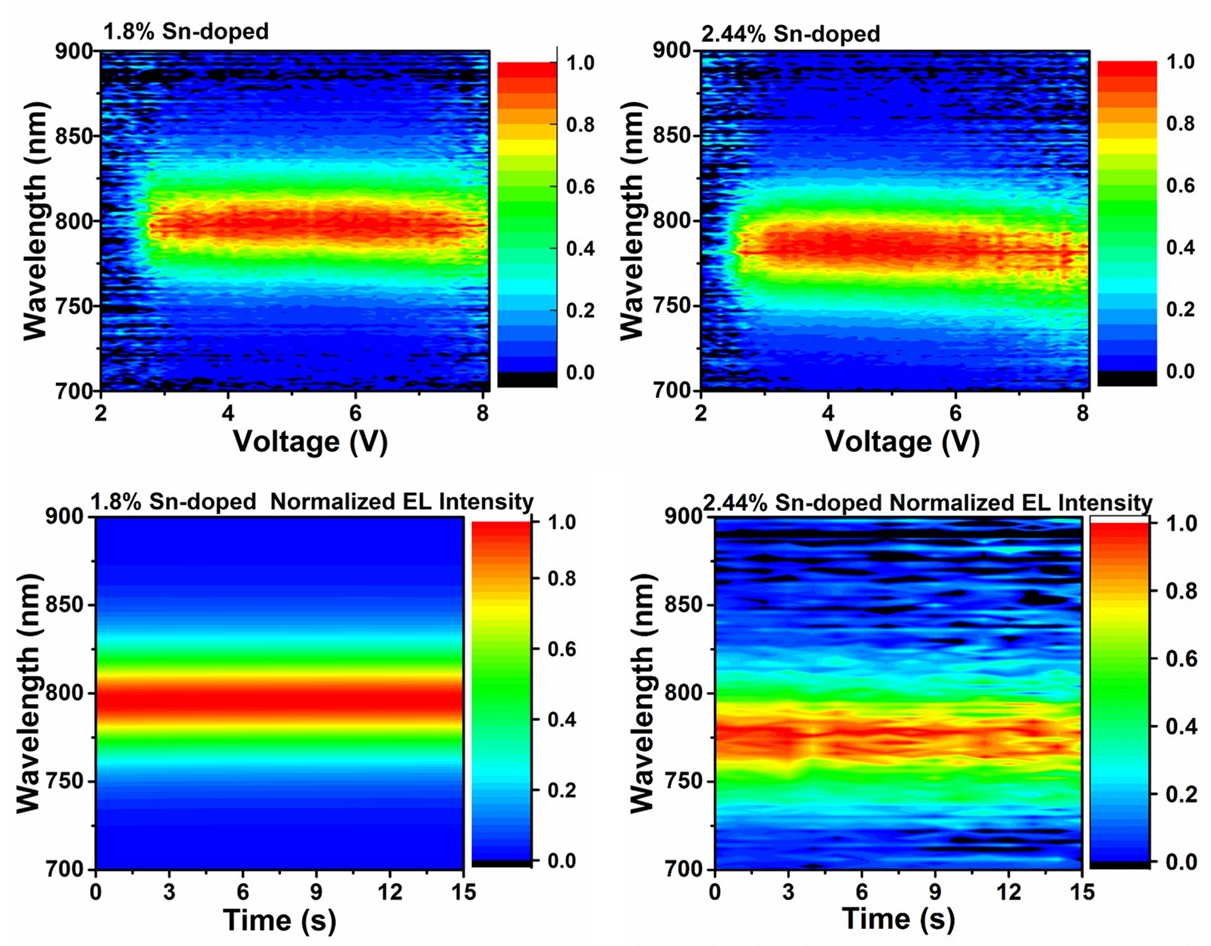

Fig. S13: Electroluminescence (EL) peak as a function of varying voltage (top panel) and time (bottom panel) for 1.8% and 2.44% Sn doped $FAPbI_3$ NCs

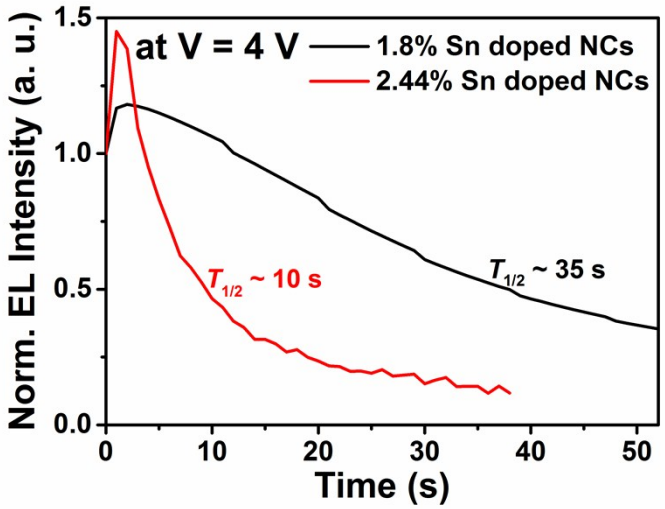

Fig. S14: EL stability at a constant bias of 4 V

LED devices were fabricated using the undoped $FAPbI_3$ NCs, however those did not turn on at all. The reason could be low quality (phase and colloidal stability), when deposited on thin film.

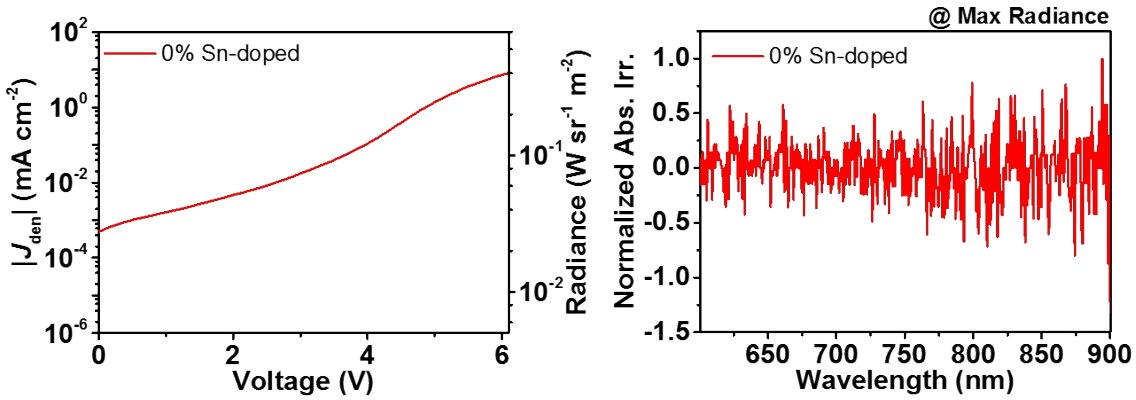

Fig. S15: (Left) Current density and radiance versus voltage (Right) EL spectra of undoped $FAPbI_3$ NCs.

REFERENCES:

[1] *ACS Nano* **2017**, *11*, 3119-3134.
[2] *Chem. Commun*. **2016**, 52, 7118.
[3] *ACS Nano* **2018**, 12, 12129.
[4] *Nat. Commun*. **2017**, 8, 996